NIH Public Access
Author Manuscript
Lasers Surg Med. Author manuscript; available in PMC 2014 July 07.

Published in final edited form as:
Lasers Surg Med. 2012 September ; 44(7): 564–571. doi:10.1002/lsm.22059.

A Fluorescence Lifetime Imaging Classification Method to Investigate the Collagen to Lipid Ratio in Fibrous Caps of Atherosclerotic Plaque

Jennifer E. Phipps, PhD[1], **Yinghua Sun, PhD**[1], **Michael C. Fishbein, MD**[2], and **Laura Marcu, PhD1**[1,*]

[1]Department of Biomedical Engineering, University of California Davis, Davis, California 95616

[2]David Geffen School of Medicine, Department of Pathology and Laboratory Medicine, University of California Los Angeles, Los Angeles, California 90095

Abstract

Background and Objective—This study describes a novel fluorescence lifetime imaging (FLIM) classification method to determine the ratio of collagen to lipid content in the fibrous cap of atherosclerotic plaques. Additionally, an analytical process to assess risk of plaque rupture based on this ratio is proposed. Collagen to lipid ratio has been shown to be an important parameter to evaluate structural integrity of the fibrous cap. FLIM and other time-resolved fluorescence techniques have recently been applied to the study of atherosclerosis based on the ability to assess biochemical composition.

Study Design/Materials and Methods—Autofluorescence of specimens retrieved during carotid endarterectomy procedures was measured through three optical filters, F377: 377/50 nm, F460: 460/66 nm, and F510: 510/ 84 nm (center wavelength/bandwidth). A Laguerre deconvolution technique was used for the evaluation of fluorescence decay dynamics. The resulting decay parameters (average fluorescence lifetime and 4 Laguerre coefficients at each of the recorded bandwidths) were used for sample characterization. Linear discriminant analysis (LDA) was used to classify each image into collagen or lipid-rich regions based on these parameters. Ultimately, a risk-level was assigned based on the ratio of collagen to lipid on the surface of the fibrous cap.

Results—FLIM images were acquired in 18 carotid plaque specimens at 43 locations. Classification of collagen and lipid-rich regions within the fibrous cap was performed with sensitivity and specificity of 80% and 82%, respectively.

Conclusions—Results from this study show that an LDA method of classifying regions of FLIM images of carotid plaque into collagen and lipid-rich regions is capable of being automated

© 2012 Wiley Periodicals, Inc.

*Corresponding to: Laura Marcu, PhD, Department of Biomedical Engineering, University of California, 1 Shields Ave., Davis, CA 95616. lmarcu@ucdavis.edu.

Conflict of Interest Disclosures: All authors have completed and submitted the ICMJE Form for Disclosure of Potential Conflicts of Interest and none were reported.

NIH-PA Author Manuscript
NIH-PA Author Manuscript
NIH-PA Author Manuscript

NIH-PA Author Manuscript

NIH-PA Author Manuscript

NIH-PA Author Manuscript

and used to rate the risk of plaque rupture based on autofluorescence decay dynamics and without the need for fluorescence intensity or contrast agents. Lasers Surg. Med. 44:564–571, 2012.

Keywords

carotid plaque; fluorescence lifetime imaging microscopy (FLIM); vulnerable plaque

INTRODUCTION

Rupture of vulnerable atherosclerotic plaque in coronary arteries is the cause of most acute coronary syndromes and myocardial infarction [1]. While clinical methods to predict presence of coronary atherosclerosis (e.g., CT angiography, coronary angiography, intravascular ultrasound (IVUS), and intravascular optical coherence tomography (OCT)) exist and are now routinely used in clinical practice, techniques to assess risk of plaque rupture are still under development [2,3]. Hallmarks of plaque vulnerability include thin fibrous cap, presence of lipid and necrosis, and inflammatory cell infiltration and are imaging targets for the identification of plaques with high-risk of rupture [4]. Several new imaging techniques are being developed to detect such features [5]. Near-infrared (NIR) fluorescence spectroscopy is capable of identifying the specific biochemical properties of lipid in the artery and is available clinically, but it does not provide depth resolved information and thus the distance of the lipid to the lumen of the artery cannot be discerned [6]. Clinically, this is significant because the closer the lipid is to the lumen, the more vulnerable the plaque is to rupture. NIR fluorescence imaging has also been used to image atherosclerosis, however these methods require exogenous contrast agents [7,8]. Thermography is a technique that identifies inflammation in the arterial wall by detecting increases in heat that are caused by inflammation [5]. Optical coherence tomography (OCT) and intravascular ultrasound (IVUS) both recognize the fibrous cap [9,10], however, another factor to consider is the presence of lipids and inflammatory cells, known to increase risk of plaque rupture by weakening the cap structure. OCT has been shown capable of identifying macrophages and lipid based on light-scattering properties, but is not specific to biochemical composition [11,12]. While IVUS is the most widespread clinically used technique for vulnerable plaque imaging, its resolution is low and its accuracy is a known disadvantage [13,14]. Additionally, a recent study has found that collagen fiber thickness affects echogenicity—thick fibers were found to be hyperechoic and thin fibers to be hypoechoic in human aortic tissue [14]. This introduces the concept that IVUS may not be completely reliable at distinguishing between lipid-rich and collagen-rich plaques.

However, in contrast, time-resolved fluorescence spectroscopy (TRFS) techniques are sensitive in detecting the collagen cross-links and therefore reliable for collagen imaging. They have also been shown capable of identifying macrophages and lipid-rich content based specifically on the biochemical makeup of these molecules, and because of the shallow penetration of light, the fibrous cap region is specifically targeted for analysis [15,16]. Thus in comparison to NIR fluorescence spectroscopy, it is able to identify shallow lipid pools indicative of increased risk of plaque rupture. TRFS is also sensitive to collagen biochemistry and thus a ratio of lipid to collagen content in the fibrous cap, significant in determining risk of plaque rupture [17], can be determined. Moreover, intravascular TRFS

NIH-PA Author Manuscript

NIH-PA Author Manuscript

NIH-PA Author Manuscript

catheters have been implemented in vivo in porcine models, and are able to acquire signal in the arterial environment since blood affects only fluorescence intensity, not time-resolved (lifetime) properties [18,19]. Fluorescence lifetime imaging (FLIM) has been developed as an extension of the TRFS technique to provide images of time-resolved properties that map the biochemical composition of regions of artery with high spatial resolution. We previously demonstrated a successful plaque characterization technique with FLIM images of human aorta (collagen, lipid, and elastin content) [20]. More recently, Park et al. [21] reported a similar scanning FLIM technique for biochemical characterization of the coronary arterial wall; implementing a classification method that identified “high-collagen,” “high-lipid,” and “low-collagen/ lipid” histopathologies based on both fluorescence intensity and lifetime. However, fluorescence intensity information is unreliable clinically due to the varying amount blood (hemoglobin) in the optical field of view as well as due to changes in the field of view and distance between catheter and arterial wall caused by movement of the catheter and heart. Both conditions can significantly affect the fluorescence intensity. Thus, a goal of this study is to determine if analysis methods that make use of parameters derived from fluorescence decay alone can be used for plaque characterization and classification. Such methods can be applied not only to data obtained using a wide-field FLIM technique but also to data obtained using a rotational-scanning FLIM pull-back technique [22]. Here we present an innovative automated classification method that uses FLIM images of human carotid artery to characterize the lipid and collagen content in fibrous caps of atherosclerotic plaques. Automation of classification techniques is imperative for clinical systems that will require real- or near-time diagnosis during intravascular procedures.

Additionally, an analytical method to determine “risk-level” based on biochemical composition is evaluated: the higher the ratio of lipid-rich composition to collagen within luminal area, the higher the risk-level. These risk levels are clinically justified because patients with a higher lipid to collagen ratio in the fibrous cap are more likely to experience heart attack [1] and experimentally justified by providing proof-of-concept that a risk-level can be determined based on the automated classification method described here. This is the first step towards implementing on-line assessment of plaque vulnerability and focuses primarily on collagen to lipid ratio. In the future, the technique is anticipated to be more robust and accurate by incorporating other features detected by fluorescence lifetime techniques (thickness of fibrous cap, macrophage infiltration/inflammation, or matrix metalloproteinase expression [16,23]). This is important for intended intravascular implementation of a scanning single-fiber FLIM system [19].

METHODS

Specimens

Plaques from 18 patients (9 female, 9 male, average age 65 ± 2.8 years) undergoing carotid endarterectomy were included in this study. All patients gave informed consent and the study was approved by the University of California Davis Institutional Review Board. FLIM images were acquired from several locations per specimen within 24 hours of surgery for a total of 43 locations. Prior to imaging, tissue was stored at 3°C in saline-soaked gauze. Each image was acquired in approximately 2 minutes and tissue was kept moist with drops of

NIH-PA Author Manuscript

NIH-PA Author Manuscript

NIH-PA Author Manuscript

saline. Imaged locations were marked with India ink and processed routinely for histological analysis.

FLIM Instrumentation

The custom designed flexible fiber bundle-based FLIM system allowed in one measurement the mapping of biochemical composition (4 mm diameter × 250 μm depth) with ~35 mm spatial resolution. Tissue autofluorescence was induced with a pulsed laser (337 nm, 700 picoseconds, MNL 205 Nitrogen, LTB Lasertechnik) and collected through a gradient index (GRIN) lens (numerical aperture: 0.5, diameter: 0.5 mm, field of view: 4 mm, GRINTECH GmbH, Jena) cemented to a fiber imaging bundle (0.6 mm in diameter, 2 m in length, 10,000 fibers). Fluorescence emitted from the proximal end of the fiber was projected onto a compact gated intensified CCD (ICCD) camera (4 Picos, Stanford Computer Optics) that achieved gating times up to 200 picoseconds. This system (Fig. 1A) is further detailed in earlier publications [20,24]. Based on previous TRFS and FLIM results from human atherosclerotic plaque [20,25], three filters were used: F377: 377/50 nm, F460: 460/60 nm, and F510/84 nm (center wavelength/bandwidth) that provide discrimination between intrinsic fluorophores related to plaque vulnerability. Collagen and elastin have peak fluorescence emission in the F377 band and are associated with normal artery and collagen-rich/stable plaques, respectively. Lipid fluorescence has peak emission at longer wavelengths, captured by the F460 band and is associated with plaques with large lipid cores and thin fibrotic caps. F510 is a new addition to this study compared to previous studies, chosen to particularly target the short average lifetimes of lipids in this region.

FLIM Measurements

Fluorescence intensity images were recorded with 0.5 nanoseconds gating time at 0.5 nanoseconds intervals for 30 nanoseconds. The fluorescence decay from each pixel in the images was retrieved through deconvolution with a Laguerre expansion technique [26,27] implemented in MATLAB. This type of deconvolution is used because (1) it estimates the fluorescence intensity decay for all pixels simultaneously, without a priori assumption of the functional form of the decay, (2) it performs at least two orders of magnitude faster than other common deconvolution algorithms, (3) Laguerre coefficients (i.e., LEC-0, 1, 2, and 3) have been associated with chemical composition [26,27]. Following Laguerre deconvolution, the average fluorescence lifetime image (t) was determined by calculating the time fluorescence intensity at each pixel decayed to 1/e of its maximum value [28]. All FLIM-derived images are false-color with pixel color representing fluorescence lifetime, intensity, or LEC values.

FLIM-Derived Parameters

Each imaged region is described by 15 FLIM-derived parameters: t_{F377}, t_{F460}, t_{F510}, and LEC-0, -1, -2, and -3 at F377, F460, and F510. Histograms of pixel values quantify information in the images.

NIH-PA Author Manuscript

NIH-PA Author Manuscript

NIH-PA Author Manuscript

Histopathological Analysis

Tissue sections 4 μm thick were stained with hematoxylin and eosin (H&E) and elastic/trichrome (trichrome) and analyzed for 0–100% of collagen, elastin, calcification, necrotic/lipid core, and number of lipid-rich macrophages, and lymphocytes per high-power field of view (HPF) within the imaged volume. Collagen fibers were stained blue in the trichrome stain, elastin fibers were stained black, lipid was identified by empty spaces in the H&E and trichrome stains where lipid washed out during processing. Lipid-rich macrophages and lymphocytes were identified by their foamy appearance in both the H&E and trichrome stained sections and necrosis was identified by the presence of cholesterol crystals inside the lipid core. Based on histopathology, three regions of interest (ROIs) were defined: (1) intimal thickening (IT: >5% elastin, 0% necrotic/lipid core, 0 macrophages/HPF), (2) lipid-rich (LR: >10 macrophages/ HPF and/or necrotic/lipid core present), and (3) collagen-rich (CR: 0% necrotic/lipid core, 0 macrophages/HPF, <5% elastin).

Two sections of tissue were used to determine ROIs for the 4 mm image; the method of inking the tissue prior to histopathological analysis allowed for an estimation of the location of each section. Parameters from features found in the region of the FLIM images corresponding to the histopathology section were used to recognize connecting and similar features.

Data Analysis and Classification

Mean and standard error (SE) of FLIM-derived parameters from each type of ROI (IT, CR, and LR) were computed and a two-tailed, unpaired *t*-test determined which parameters varied with statistical significance between groups. After an initial assessment of the data-set, it was found that the group of IT specimens was too small to be used in a classification scheme. Thus they are subsequently left out of the remaining data processing methods. First, ROIs were selected from each image that directly corresponded to histology sections. Next, pixels in the ROIs were binned into 10 × 10 blocks and classified as CR or LR with linear discriminant analysis (LDA) and leave-one-out cross-validation (LOOCV). LOOCV was used in this study because of the limited amount of data that had a direct correlation with histology sections (two tissue sections per FLIM image). With a larger study or more histology sections, separate training, and validation sets could be used. In this case, LOOCV was used for the FLIM pixels directly corresponding to a histology section, then that set was used as a separate training set with the remaining pixels as the validation set. Thus the ROIs from a single image were left out of the training set and then tested based on histology and FLIM-derived parameters from pixels in remaining images; this procedure was performed sequentially for each image. Sensitivity and specificity were calculated for this step (Fig. 1B, path i). Next the pixels that were validated with the LOOCV technique were used as a training set to classify the rest of the image that did not have corresponding histopathology in 10 × 10 blocks. Lastly, surface area of each biochemical component was calculated and an overall risk-level was assigned to the imaged region, separate from the classification of the individual ROIs (Fig. 1B, path ii).

NIH-PA Author Manuscript

NIH-PA Author Manuscript

NIH-PA Author Manuscript

Risk Levels

Three levels of risk were defined for this study, but this could be a flexible parameter, dependent on the most current definition of plaque instability and the arterial bed being imaged. A necrotic core at least 2 mm long is defined as an indicator of a vulnerable plaque in coronary arteries [29] thus 4 mm^2 was defined as a surface area that could indicate a necrotic core at least 2 mm long. Following are the three risk levels defined for this study, level 1: >20% CR, 0% LR, a collagen-rich, likely stable plaque; level 2: 10–50% LR and LR surface area <4 mm^2, possible the edge of a lipid pool or a small lipid pool; and level 3: >50% LR or LR surface area >4 mm^2, likely a high-risk plaque.

In this study, risk-level is referring only to the limited depth of tissue (~250 μm) investigated, so it is a surface specific indicator, not relevant for the entire plaque type. However, in conjunction with a morphological imaging technique, such as IVUS or OCT, this risk-level could be extended to overall plaque type.

RESULTS

Eighty-five ROIs were identified from 43 FLIM-imaged locations, IT (*n* = 9), CR (*n* = 33), and LR (*n* = 43).

FLIM-Derived Parameters

Pixels within IT ROIs varied significantly from CR and LR cases, except for LEC-0_{F460}, LEC-1_{F510}, and LEC-3_{F510}. However, because samples in this study were most often fully developed plaques, there were few IT specimens and data from this group was excluded from the classification. All parameters varied significantly between pixels in CR and LR ROIs. Average FLIM-derived parameters SE are provided (Table 1). CR regions were identified by longer lifetimes compared to LR regions: 1.90 ± 0.01 nanoseconds versus 1.56 ± 0.01 nanosec- nanoseconds, respectively (F510). CR regions also exhibited negative LEC-1 values compared to the positive values in LR regions: —0.02 ± 0.00 versus 0.02 ± 0.00, respectively (F377).

Classification of ROIs

The 76 ROIs (not including IT specimens) were classified with sensitivity: 80% and specificity: 82% when using the entire dataset (15 FLIM-derived parameters). The rank of significance of each parameter in the classification is listed in Table 1. Rank is interesting to look at because small changes in FLIM-derived parameters can become statistically significant with large numbers of pixels, but the parameters with the greatest variation between groups were weighted more heavily in the classification algorithm. For example, t_{F377} is ranked 14 (2nd from the least significant) despite varying between groups by ~0.4 nanoseconds and LEC-1_{F377} is ranked 2 (2nd from most significant) while varying only 0.04 between groups. Thus LEC-1_{F377} is a stronger classifier between LR and CR composition than t_{F377}. Classification of each image required less than 1 minute.

NIH-PA Author Manuscript

NIH-PA Author Manuscript

NIH-PA Author Manuscript

Risk-Level

Each image was assigned a risk-level based on percentage and dimensions of surface area covered by each biochemical constituent: level 1 (n = 13), level 2 (n = 5), and level 3 (n = 25). Compared to current clinical plaque classification methods [4], risk-level 1 would imply a stable plaque or an artery with intimal thickening (pathological or intimal xanthoma), risk-level 2 is a fibroatheroma or the edge of a thin-cap fibroatheroma, risk-level 3 is a thin-cap fibroatheroma (the most likely to rupture of the three levels).

Figure 2 depicts examples of details of the classification process. Representative FLIM-derived parameters (t_{F377}, LEC-1_{F377}, and LEC-1_{F460}) and histograms that quantify differences in the pixel values of the parameters are shown. The red and blue circles represent ROIs depicted in histograms for LR and CR regions, respectively. Pixels outside of the red and blue-circled ROIs that have no corresponding histology information were assigned a group based on the LDA classification of averaged FLIM-derived parameters from each 10 × 10 pixel block. Then overall classification into CR and LR components was used to define a risk-level: level 2 for the left panel (Fig. 2E), level 3 for the right panel (Fig. 2J).

DISCUSSION

This study has shown for the first time that a ratio of collagen to lipid content of the fibrous cap of atherosclerotic plaque can be determined with a FLIM technique in an automated manner. Improvements were made compared to previous time-resolved methods of analyzing athero-sclerotic plaque by incorporating a clinically translatable analytical algorithm that assigns a risk-level based on the surface area of each fibrous cap covered by collagen and lipid-rich tissue. The capability of automating image processing and risk assessment is important as our group continues to work towards clinical translation of FLIM techniques for plaque characterization.

Determining Lipid to Collagen Ratio With FLIM

Fluorophores in the artery and plaque dominate fluorescence decay dynamics of each FLIM measurement (IT: elastin, CR: collagen, and LR: lipids); however, varying percentages of each component in the imaging volume will affect overall average time-resolved signal per pixel. Thus, values of average lifetimes and Laguerre coefficients may vary slightly from previously published data as well as from other pixels in the same groups in this study. The availability of 15 time-resolved parameters allows for accurate classification of each pixel as collagen or lipid-dominant despite some variability in the individual parameters. For example, the CR average lifetime values were longer than all other groups (2.06 nanoseconds at F377), but shorter than many values defined in the literature (3–4 nanoseconds at 390 nm) [30], and LR t_{F377} values were similar to the IT group, but distinguished by shorter values at t_{F460} and t_{F510} because of short lifetimes of lipid (data not shown) [15]. Laguerre coefficients are equally important as average lifetime to the pixel classification method. LEC-1 and -3 were found to vary most significantly between collagen and lipid-dominant regions because LEC-3 captures the dynamics of the faster decay times of elastin and lipid whereas LEC-1 captures the dynamics of the slower decay times of

NIH-PA Author Manuscript

NIH-PA Author Manuscript

NIH-PA Author Manuscript

collagen, which is in agreement with a previous study [20]. Increased sensitivity to fluorescence decay dynamics exhibited by the Laguerre coefficients has been noted in other time-resolved plaque studies as well [16,20], this is another advantage to time-resolved autofluorescence studies that use a Laguerre deconvolution technique to retrieve lifetime information.

Risk-Level

FLIM is capable of assessing biochemical composition at the arterial intimal surface (fibrous cap), but it cannot assess stenosis or outward remodeling. However, combining FLIM with an imaging modality that also assessed plaque burden such as IVUS or OCT [18,31] would enhance the diagnostic capabilities of a FLIM technique. Thus the three risk levels defined here were a demonstration of how a FLIM technique could classify an image into one of several levels of risk based only on the size and percentage of surface area covered by CR and LR biochemical compositions. Many imaging studies classify plaque based on Virmani et al. [4] modified American Heart Association definitions, which could be built in to the risk-level assessment if FLIM is combined with an imaging modality that can also assess plaque stenosis, outward remodeling, and lipid cores deeper in the tissue than the 250 μm depth imaging volume. Currently our group is developing such a system that would combine a FLIM technique with IVUS [18]. The ability to determine the lipid content in the several 100 μm of tissue nearest to the lumen of the artery and to provide an assessment of the risk of rupture based on this information will be important for current cardiac catheterization imaging techniques.

Study limitations—The choice of carotid plaque as a model for this study was made because the samples can be retrieved quickly after surgery allowing for fluorescence emission assessment of sample biochemistry while the tissue is fresh. However, the drawback of using carotid plaque is that the tissue is very diseased hence limited data from normal tissue or early atherosclerotic lesions was acquired. With a larger data set from carotid plaques or with the addition of data from coronary or aortic arteries where normal tissue or early plaques are more often found, this technique could be used to determine plaque biochemical composition with varying percentages of collagen, elastin, lipids, and macrophages and thus determine an even more accurate level of risk of plaque rupture. Additionally, an overall assessment of inflammation in the samples was not performed aside from identification of macrophages based on their appearance in H&E and trichrome stained tissue sections. Inflammation is an important indicator of plaque vulnerability and since TRFS has detected inflammation in previous studies [15,16], it will be important to add this capability to improve the accuracy of this technique for predicting risk of plaque rupture. Lastly, clinical implementation of a whole-field FLIM system is not practical due to the lengthy image acquisition times. To address this limitation, in a parallel study we developed a scanning system allowing for fast image acquisition in an intraluminal setting in rotational and pull-back mode [22]. This system also allows single-fiber implementation in a catheter small enough for intravascular use that can also incorporate a blood flushing system [19]. The classification algorithm based on fluorescence decay parameters rather than intensity developed here will be adapted to the scanning system for clinical application.

NIH-PA Author Manuscript

NIH-PA Author Manuscript

NIH-PA Author Manuscript

CONCLUSION

FLIM characterization of lipid and collagen content in atherosclerotic plaques is unique compared to other imaging modalities since the FLIM signal is generated by the molecular composition of the fibrous cap (due to shallow penetration depth). This allows for robust assessment of lipids and lipid-rich macrophages near the intimal surface to assess risk of plaque rupture, particularly when combined with other imaging techniques such as angioscopy, IVUS, or OCT. Moreover, FLIM images can be acquired with a pullback motion through a rotational single-fiber catheter, currently in development [18]. The capability of performing this analysis without user input is necessary for the intended clinical implementation of a similar TRF imaging technique [19] and for increasing ease of use during studies leading up to clinical translation. Time-resolved studies have already found great success in the characterization of plaque biochemical composition and the development of this novel classification method to determine lipid to collagen ratio in the fibrous cap and subsequently perform a risk assessment analysis further increases the potential of such systems for clinical translation.

Acknowledgments

The authors would like to thank Matthew Lam for his assistance throughout the study. We also acknowledge our funding sources: The National Institutes of Health R01 HL 67377 (to L.M.) and Howard Hughes Medical Institute Med-Into-Grad Fellowship at UC Davis (to J.E.P.).

Contract grant sponsor: The National Institutes of Health; Contract grant number: R01 HL 67377; Contract grant sponsor: Howard Hughes Medical Institute Med-Into-Grad Fellowship.

REFERENCES

1. Virmani R, Burke AP, Farb A, Kolodgie FD. Pathology of the vulnerable plaque. J Am Coll Cardiol. 2006; 47(8 Suppl):C13–C18. [PubMed: 16631505]
2. Sharif F, Murphy RT. Current status of vulnerable plaque detection. Catheter Cardiovasc Interv. 2010; 75(1):135–144. [PubMed: 19670307]
3. Schaar JA, Mastik F, Regar E, den Uil CA, Gijsen FJ, Went-zel JJ, Serruys PW, van der Stehen AFW. Current diagnostic modalities for vulnerable plaque detection. Curr Pharm Des. 2007; 13(10):995–1001. [PubMed: 17430163]
4. Virmani R, Kolodgie FD, Burke AP, Farb A, Schwartz SM. Lessons from sudden coronary death—A comprehensive morphological classification scheme for atherosclerotic lesions. Arteriosc Thromb Vasc Biol. 2000; 20(5):1262–1275.
5. Vancraeynest D, Pasquet A, Roelants V, Gerber BL, Vanoverschelde JL. Imaging the vulnerable plaque. J Am Coll Cardiol. 2011; 57(20):1961–1979. [PubMed: 21565634]
6. Waxman S, Dixon SR, L'Allier P, Moses JW, Petersen JL, Cutlip D, Tardif JC, Nesto RW, Muller JE, Hendricks MJ, Sum ST, Gardner CM, Goldstein JA, Stone GW, Krucoff MW. In vivo validation of a catheter-based near-infrared spectroscopy system for detection of lipid core coronary plaques: Initial results of the SPECTACL study. JACC Cardiovasc Imaging. 2009; 2(7):858–868. [PubMed: 19608137]
7. Yoo H, Kim JW, Shishkov M, Namati E, Morse T, Shubochkin R, McCarthy JR, Ntziachristos V, Bouma BE, Jaffer FA, Tearney GJ. Intra-arterial catheter for simultaneous micro-structural and molecular imaging in vivo. Nat Med. 2011; 17(12):1680–1684. [PubMed: 22057345]
8. Calfon MA, Vinegoni C, Ntziachristos V, Jaffer FA. Intravascular near-infrared fluorescence molecular imaging of atherosclerosis: Toward coronary arterial visualization of biologically high-risk plaques. J Biomed Opt. 2010; 15(1):011107. [PubMed: 20210433]

NIH-PA Author Manuscript

NIH-PA Author Manuscript

NIH-PA Author Manuscript

9. Mintz GS, Maehara A. Serial intravascular ultrasound assessment of atherosclerosis progression and regression. State-of-the-art and limitations. Circ J. 2009; 73(9):1557–1560. [PubMed: 19638706]
10. Jang IK, Tearney GJ, MacNeill B, Takano M, Moselewski F, Iftima N, Shishkov M, Houser S, Aretz HT, Halpern EF, Bouma BE. In vivo characterization of coronary atherosclerotic plaque by use of optical coherence tomography. Circulation. 2005; 111(12):1551–1555. [PubMed: 15781733]
11. Tearney GJ, Yabushita H, Houser SL, Aretz HT, Jang IK, Schlendorf KH, Kauffman CR, Shishkov M, Halpern EF, Bouma BE. Quantification of macrophage content in athero-sclerotic plaques by optical coherence tomography. Circulation. 2003; 107(1):113–119. [PubMed: 12515752]
12. Yabushita H, Bouma BE, Houser SL, Aretz HT, Jang IK, Schlendorf KH, Kauffman CR, Shishkov M, Kang DH, Halpern EF, Tearney GJ. Characterization of human atherosclerosis by optical coherence tomography. Circulation. 2002; 106(13):1640–1645. [PubMed: 12270856]
13. Thim T, Hagensen MK, Wallace-Bradley D, Granada JF, Kaluza GL, Drouet L, Paaske WP, Botker HE, Falk E. Unreliable assessment of necrotic core by virtual histology intravascular ultrasound in porcine coronary artery disease. Circ Cardiovasc Imaging. 2010; 3(4):384–391. [PubMed: 20460496]
14. Tabel GM, Hepel J, Whittaker P, Palal B, Chandraratna PA. Hypoechoic areas on ultrasound images of atheroma are not always diagnostic of fatty plaque. Ultrasound Med Biol. 2005; 31(8): 1013–1015. [PubMed: 16085091]
15. Marcu L, Fang QY, Jo JA, Papaioannou T, Dorafshar A, Reil T, Qiao JH, Baker JD, Freischlag JA, Fishbein MC. In vivo detection of macrophages in a rabbit atherosclerotic model by time-resolved laser-induced fluorescence spectroscopy. Atherosclerosis. 2005; 181(2):295–303. [PubMed: 16039283]
16. Marcu L, Jo JA, Fang Q, Papaioannou T, Reil T, Qiao JH, Baker JD, Freischlag JA, Fishbein MC. Detection of rupture-prone atherosclerotic plaques by time-resolved laser-induced fluorescence spectroscopy. Atherosclerosis. 2009; 204(1):156–164. [PubMed: 18926540]
17. Neumeister V, Scheibe M, Lattke P, Jaross W. Determination of the cholesterol-collagen ratio of arterial atherosclerotic plaques using near infrared spectroscopy as a possible measure of plaque stability. Atherosclerosis. 2002; 165(2):251–257. [PubMed: 12417275]
18. Stephens DN, Park J, Sun Y, Papaioannou T, Marcu L. Intraluminal fluorescence spectroscopy catheter with ultra-sound guidance. J Biomed Opt. 2009; 14(3):030505. [PubMed: 19566287]
19. Sun Y, Stephens D, Xie H, Phipps J, Saroufeem R, Southard J, Elson DS, Marcu L. Dynamic tissue analysis using time- and wavelength-resolved fluorescence spectroscopy for atherosclerosis diagnosis. Opt Express. 2011; 19(5):3890–3901. [PubMed: 21369214]
20. Phipps JE, Sun Y, Saroufeem R, Hatami N, Fishbein MC, Marcu L. Fluorescence lifetime imaging for the characterization of the biochemical composition of atherosclerotic plaques. J Biomed Opt. 2011; 16(9):096018. [PubMed: 21950932]
21. Park J, Pande P, Shrestha S, Clubb F, Applegate BE, Jo JA. Biochemical characterization of atherosclerotic plaques by endogenous multispectral fluorescence lifetime imaging microscopy. Atherosclerosis. 2012; 220(2):394–401. [PubMed: 22138141]
22. Xie H, Bec J, Liu J, Sun Y, Lam M, Yankelevich D, Marcu L. Multispectral scanning time-resolved fluorescence spectroscopy (TRFS) technique for intravascular diagnosis. Biomed Opt Express. 2012; 3(7):1521–1533. [PubMed: 22808425]
23. Phipps JE, Hatami N, Galis ZS, Baker JD, Fishbein MC, Marcu L. A fluorescence lifetime spectroscopy study of matrix metalloproteinases-2 and -9 in human atherosclerotic plaque. J Biophot. 2011; 4(9):650–658.
24. Sun Y, Phipps J, Elson DS, Stoy H, Tinling S, Meier J, Poirier B, Chuang FS, Farwell DG, Marcu L. Fluorescence lifetime imaging microscopy: In vivo application to diagnosis of oral carcinoma. Opt Lett. 2009; 34(13):2081–2083. [PubMed: 19572006]
25. Marcu L, Jo JA, Fang Q, Papaioannou T, Reil T, Qiao JH, Baker JD, Freischlag JA, Fishbein M. Detection of rupture-prone atherosclerotic plaques by time-resolved laser-induced fluorescence spectroscopy. Atherosclerosis. 2008:10552.

NIH-PA Author Manuscript

NIH-PA Author Manuscript

NIH-PA Author Manuscript

26. Jo JA, Fang Q, Marcu L. Ultrafast method for the analysis of fluorescence lifetime imaging microscopy data based on the laguerre expansion technique. IEEE J Quantum Electron. 2005; 11(4):835–8845. [PubMed: 19444338]

27. Jo JA, Fang QY, Papaioannou T, Marcu L. Fast model-free deconvolution of fluorescence decay for analysis of biological systems. J Biomed Opt. 2004; 9(4):743–752. [PubMed: 15250761]

28. Lakowicz, JR. Principles of fluorescence spectroscopy. Springer; New York: 1999. p. 698

29. Virmani R, Malik S, Burke A, Skorija K, Wong N, Kolodgie F, Narula J. Vulnerable plaque pathology for imagers. Circulation. 2006; 114(18):385–385.

30. Marcu, L.; Grundfest, WS.; Fishbein, M. Time-resolved laser-induced fluorescence spectroscopy for staging atherosclerotic lesions.. In: Mycek, MA.; Pogue, BW., editors. Handbook of biomedical fluorescence. New York: Marcel Dekker, Inc.. 2003. p. 397-430.

31. Park J, Jo JA, Shrestha S, Pande P, Wan Q, Applegate BE. A dual-modality optical coherence tomography and fluorescence lifetime imaging microscopy system for simultaneous morphological and biochemical tissue characterization. Biomed Opt Express. 2010; 1(1):186–200. [PubMed: 21258457]

NIH-PA Author Manuscript
NIH-PA Author Manuscript
NIH-PA Author Manuscript

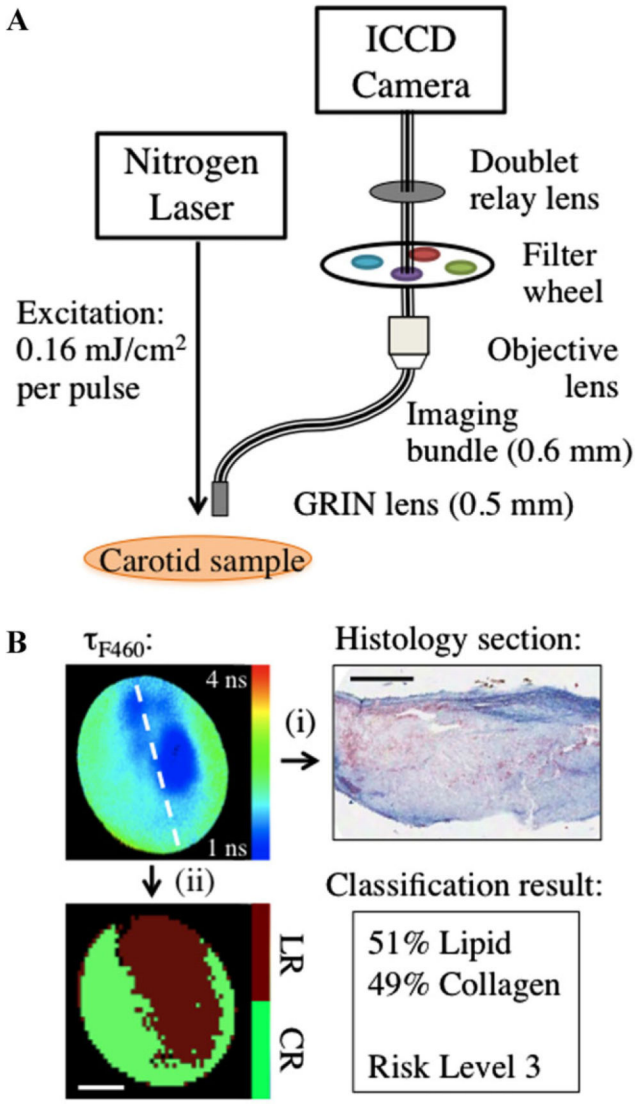

Fig. 1.

A: Schematic of FLIM instrumentation. **B:** Representative example of risk assessment process: (i) histology sections from the center of FLIM images (white dashed line in FLIM image) are used to identify collagen-rich and lipid-rich regions and (**ii**) based on co-registration with histology (ink marks on tissue section), classification is performed to identify collagen-rich versus lipid-rich surface area and to assign risk-level. Scale bars are 1 mm.

NIH-PA Author Manuscript
NIH-PA Author Manuscript
NIH-PA Author Manuscript

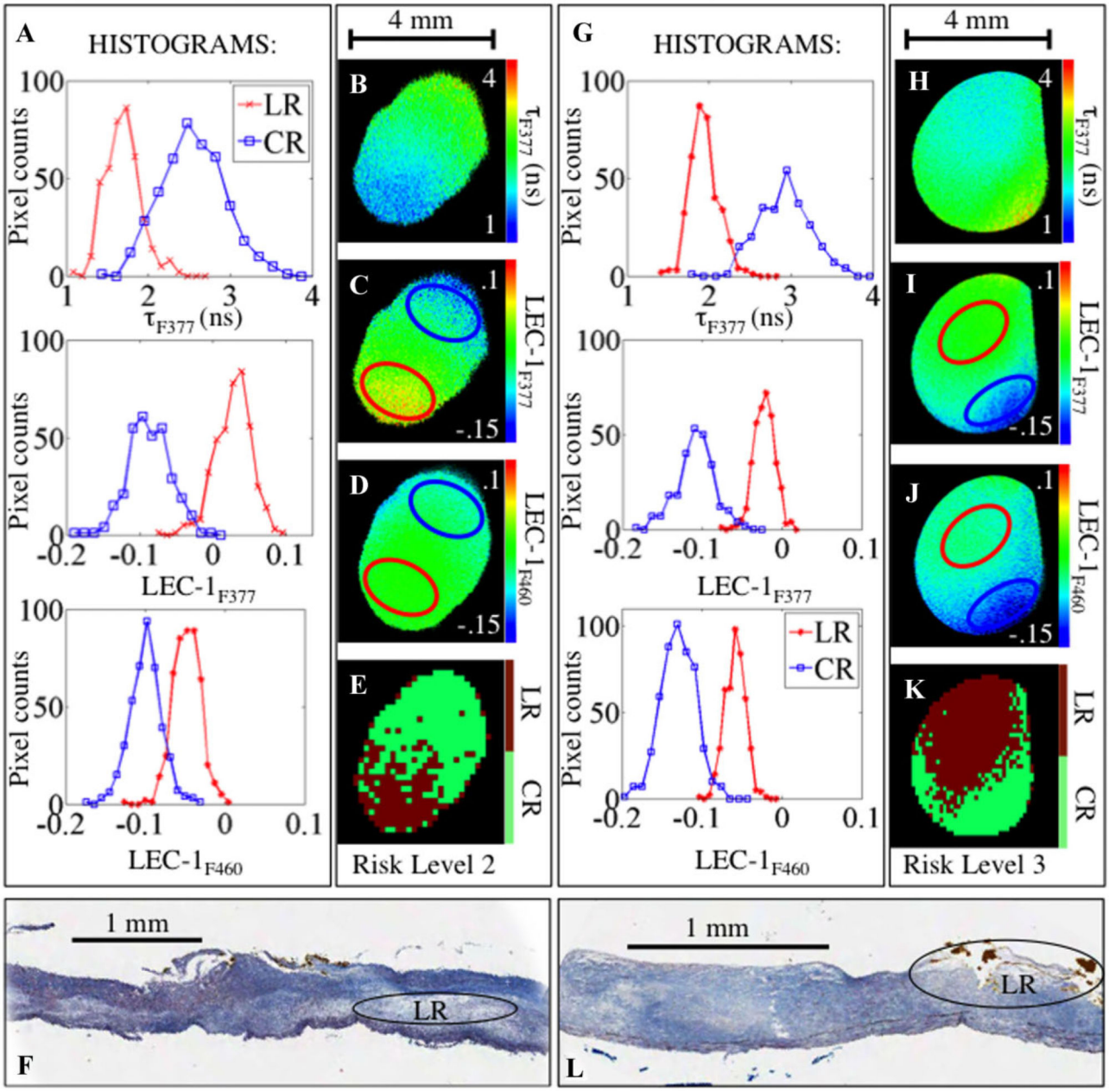

Fig. 2.

A and **G:** Histograms from images in (**B–D**), and (**H–J**), respectively. B and H: t_{F377}. **C.** and **I**: LEC-1_{F377}. D and J: LEC-1_{F460}. Blue circle: CR region, red circle: LR region. Histograms from pixels within these regions are plotted in (A) and (F). E and **K:** Classification of entire image. F and **L:** Trichrome stained tissue sections from FLIM data shown in (A–E) and (**G–K**), respectively. Lipid pools are seen in both images, circled and labeled “LR.”

NIH-PA Author Manuscript

NIH-PA Author Manuscript

NIH-PA Author Manuscript

TABLE 1

Average FLIM-Derived Parameters ± SE for Each Type of ROI at Each Bandwidth Assessed, *P* Values Indicating Statistical Significance, and Rank of Each Parameter in the Classification Algorithm (1 is Most Significant, 15 Is Least Significant).

Band	Collagen-rich	Lipid-rich	P-value	Rank
Average lifetime				
F377	2.06±0.01	1.63±0.01	<0.001	14
F460	1.99±0.01	1.68±0.01	<0.001	11
F510	1.90±0.01	1.56±0.01	<0.001	8
LEC-0				
F377	0.81±0.00	0.76±0.00	<0.001	5
F460	0.79±0.00	0.77±0.00	<0.001	4
F510	0.79±0.00	0.75±0.00	<0.001	3
LEC-1				
F377	–0.02±0.00	0.02±0.00	<0.001	2
F460	–0.04±0.00	0.00±0.00	<0.001	6
F510	–0.03±0.00	0.00±0.00	<0.001	7
LEC-2				
F377	0.11±0.00	0.13±0.00	<0.001	9
F460	0.13±0.00	0.14±0.00	<0.001	12
F510	0.13±0.00	0.16±0.00	<0.001	10
LEC-3				
F377	0.02±0.00	0.06±0.00	<0.001	1
F460	0.02±0.00	0.04±0.00	<0.001	13
F510	0.03±0.00	0.04±0.00	<0.001	15